Influence of Rhenium as an Alloying Element on the Pitting Corrosion Behaviour of Cast TiNiRe Shape Memory Alloys – I

Mohammed A. Amin[1,2,], Nader El-Bagoury[1,3], Adel A. Omar[4,5] and Adel S. Megahed[1]*

[1] Materials and Corrosion Lab, Chemistry Department, Faculty of Science, Taif University, 888 Hawiya, Saudia Arabia
[2] Chemistry Department, Faculty of Science, Ain Shams University, P.O. Box 11566, Abbassia, Cairo, Egypt.
[3] Casting Technology Lab., Manufacturing Technology Dept., Central Metallurgical Research and Development Institute, CMRDI, P. O. Box 87 Helwan, Cairo, Egypt.
[4] Mechanical Engineering Department, Faculty of Engineering, Taif University, Kingdom of Saudi Arabia
[5] On leave from Mechanical Engineering Department, Benha Faculty of Engineering, Benha University, Egypt
[*]E-mail: maaismail@yahoo.com

In recent years, there has been growing interest in the use of TiNi shape memory alloys (SMAs) as functional/smart materials for a variety of applications. In this study, $(Ti_{51}Ni_{49-x}Re_x)$ shape memory alloy has been modified by adding various amounts of rhenium (Re) (x = 0, 0.1 and 0.3 %) at the expense of Ni. As a first step towards studying the effect of Re (as an alloying element) on the microstructure, phase transformation, mechanical properties and uniform and pitting corrosion processes of the three tested $(Ti_{51}Ni_{49-x}Re_x)$ shape memory alloys, we have reported the results of cyclic polarization measurements on passivity breakdown and initiation and propagation of pits on the surfaces of the three tested alloys in aerated neutral 0.05 M KBr solution. The potentiodynamic anodic polarization curves of the three tested alloys exhibited no active dissolution region due to spontaneous passivation. The passive region is followed by pitting corrosion as a result of breakdown of the passive film induced by Br^- anions. Cyclic polarization measurements allow the pitting potential (E_{pit}) and the repassivation potential (E_{rp}) to be determined. E_{pit} increased with increase in Re content in the tested samples. Pitting morphology studies showed that the severity of pitting attack suppressed upon alloying $Ti_{51}Ni_{49}$ shape memory alloy with Re. These findings demonstrated that the presence of Re enhanced the pitting corrosion resistance of the tested alloys to an extent depending on the Re content. ICP-AES (inductively coupled plasma atomic emission spectrometry) was also employed as an independent method of chemical analysis to confirm results obtained from cyclic polarizations measurements.

Keywords: TiNi shape memory alloys; Alloyed rhenium; Pitting corrosion; KBr solution; Morphology of pitting

1. INTRODUCTION

Shape memory alloys (SMAs) belong to a group of functional, smart materials with the unique property of ''remembering'' the shape they had before pseudoplastic deformation. Such an effect is based on crystallographic reversible thermo-elastic martensitic transformation. Due to these characteristics and super elasticity, SMAs, especially those of Ni and Ti, have attracted considerable attention as materials for medical devices such as guide wires, stents, filters, catheters, implants and others [1–3].

In general, Ti and Ti-base alloys exhibit excellent corrosion resistance due to a strongly adherent, highly insoluble passive film formed spontaneously on the surface. It is widely agreed that the passive film consists of an outer hydroxide layer and an inner oxide layer, the latter being a main contributor to corrosion resistance [4]. These materials are therefore in a passive state at the open-circuit potential. When the potential shifts in the positive direction, almost the entire current passed is consumed by the anodic oxide film growth. However, at a rather high potential and in the presence of activation (aggressive) anions, as halides, the breakdown of passivity may occur [5-13]. Ti-base alloys have many commercial applications, which require a high resistance against pitting, or conversely, the breakdown of passivity is used to obtain a high rate of electrochemical dissolution [14].

This paper describes one part (the 1st part) of a four-part series, the objectives of which were to study the effect of Re (as an alloying element) on the microstructure, phase transformation, mechanical properties and uniform and pitting corrosion processes of a $Ti_{51}Ni_{49}$ SMA in an aggressive Br^- environment. The goal of this part is to throw more light on the specific role that Re (as an alloying element) plays on passivity and passivity breakdown, and hence the initiation of pitting corrosion, of the tested SMAs in KBr solutions. Measurements were carried out with the use of cyclic polarization measurements. An independent method of chemical analysis (ICP-AES) was also employed to determine the concentration of Ni^{2+} in solution due to pitting corrosion of the tested alloys in KBr solutions. The aim of the ICP method is to clarify the effect of Re on the rate of pitting attack and to confirm cyclic polarization measurements. Morphologies of pitted surfaces were investigated as a function of Re content in the tested SMAs.

2. EXPERIMENTAL

The SMAs used in this work were double melted and casted under vacuum, using a Skull Induction Vacuum (SIM) melting furnace. In the second melt, different amounts of Re, as an alloying element, were added to adjust the atomic chemical composition. Then a third melting process was made to ensure entirely melting and homogeneous distribution of all alloying elements in the heat. Pouring of heats was carried out into an investment casting ceramic mold. This mold was preheated to 1000 ºC before the pouring process. A quantitative chemical analysis of these alloys was performed by using electron probe micro-analyzer equipped with a wavelength dispersive X-ray spectrometer analysis system. The composition of these alloys are; Ti_{51}-Ni_{49}, Ti_{51}-$Ni_{48.9}$-$Re_{0.1}$ and Ti_{51}-$Ni_{48.7}$-$Re_{0.3}$ (atom. %). These alloys were cast as cylindrical rods for the electrochemical tests. These rods were

machined carefully and mounted in polyester resin after the electric contact, with special care taken to prevent the presence of crevices. The exposed area was ~ 1.0 cm^2. Before each run, the samples were wet ground with 600-grit silicon carbide (SiC) paper, washed in distilled water, and immersed in the electrochemical cell. The samples were then subjected to open circuit conditions until a steady state potential was reached. This procedure was accomplished in 60 min and the potential value obtained was considered the corrosion potential (E_{corr}).

All chemical and electrochemical tests were performed in 0.05 M KBr solution, as the corrosive medium, prepared with analytical grade chemicals and doubly distilled water. The solution was naturally aerated and the temperature was held at 25 ◦C using a temperature control water bath. A conventional electrochemical cell was used, consisting of a platinum counter electrode and Ag/AgCl reference electrode. A Luggin–Haber capillary was also included in the design. The tip of the Luggin capillary is made very close to the surface of the working electrode to minimize IR drop. In order to avoid Cl$^-$ diffusion in the cell, the reference electrode was connected to the working electrode through a bridge filled with the solution under test, the capillary tip of the bridge was very close to the surface of the working electrode to minimize the IR drop. In addition, Cl$^-$ ion was potentiometrically detected in the test solution before and after each polarization experiment using an Ag/AgCl selective electrode and a standard solution of AgNO$_3$ and a HANNA pH-meter model pH 211. The aim is to make sure that the pitting attack originates only from Br$^-$ anions. In all cases, the obtained results revealed the absence of Cl$^-$ ion in the tested solution.

The electrochemical cell was connected to a potentiostat; Autolab frequency response analyzer (FRA) coupled to an Autolab Potentiostat/Galvanostat (PGSTAT30) with FRA2 module connected to a personal computer. Pitting corrosion induced by the aggressive attack of Br$^-$ anion has been evaluated in terms of passivity breakdown and both nucleation of pits and growth of pre-existing pits, using cyclic polarization measurements. Such measurements were carried out by sweeping linearly the potential from the starting potential into the positive direction at a given scan rate till a required potential value and then reversed with the same scan rate till the starting potential to form one complete cycle.

For studying the influence of alloyed Re on the morphology of pitting, the three tested samples were exposed to pitting attack in 0.05 M KBr solution at a constant applied anodic potential (E_a) that exceeds their pitting potential values. Each sample was held at the given potential for 5.0 min, and finally washed thoroughly and submitted to 20 min of ultrasonic cleaning in order to remove loosely adsorbed ions. The morphology of the electrode surface was then examined using an Analytical Scanning Electron Microscope JEOL JSM 6390 LA.

The resultant solutions (i.e., the three solutions obtained after holding each alloy of the three tested alloys at E_a for 5.0 min) were used for evaluation of the rate of pitting corrosion via determination of Ni^{2+} released. The amount of nickel released into the corrosive medium was taken as a measure of the pitting corrosion rate. In this respect, an independent method of chemical analysis, namely ICP-AES was employed, using Perkin–Elmer Optima 2100 Dual View inductively coupled plasma atomic emission spectrometry (ICP-AES) instrument connected with AS 93 Plus autosampler.

3. RESULTS AND DISCUSSION

Fig. 1 shows cyclic polarization plots recorded for the three tested (Ti$_{51}$Ni$_{49-x}$Re$_x$) shape memory alloys (x = 0, 0.1 and 0.3) in 0.05 M KBr solution at a scan rate of 1.0 mV s^{-1} at 25 ∘C.
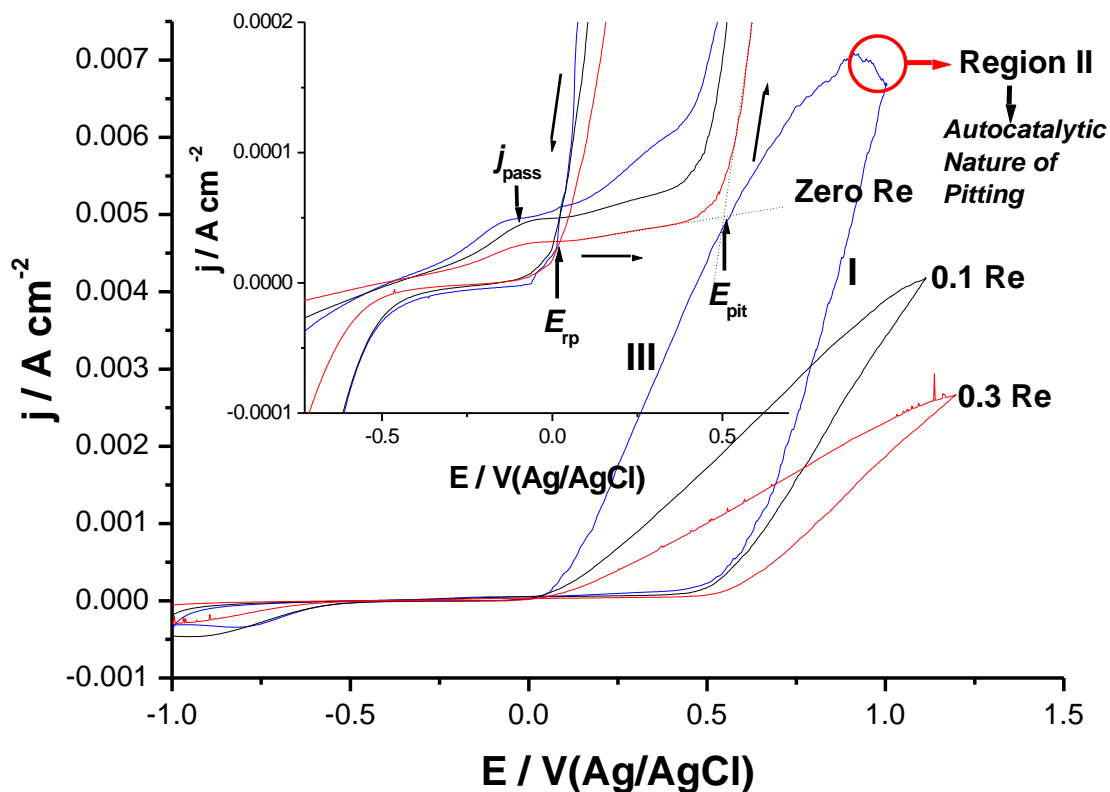
Figure 1. Cyclic polarization plots recorded for the three tested (Ti$_{51}$Ni$_{49-x}$Re$_x$) shape memory alloys (x = 0, 0.1 and 0.3) in 0.05 M KBr solution at a scan rate of 1.0 mV s^{-1} at 25 ∘C.

For all tested alloys, the anodic excursion span does not exhibit an active dissolution up to the potential corresponding passivity breakdown and initiation of pitting corrosion, namely the pitting potential (E_{pit}). The lack of active dissolution may be attributed to spontaneous passivation of the TiNi SMAs [14]. These results demonstrate that the passive film is stable in this range of potential.

The insert of Fig. 1 focuses on the region of passivity and its breakdown as a function of alloy composition. It is obvious that the passive current density, j_{pass}, decreases with increase in %Re in the tested samples, and a slight increase in j_{pass} with applied potential is observed in all cases. The decrease in j_{pass} with increase in alloyed Re content reflects, for the first sight, the increased resistance of Re-containing SMAs alloys towards pitting attack. On the other hand, the increase of j_{pass} with potential could be attributed to general weakness and thinning of the passive film as a result of the adsorption of the aggressive Br$^-$ anions on the oxide surface. EDX examinations of the electrode surface confirmed

such adsorption, see later. This adsorption is expected to enhance as applied potential made more positive.

These results reveal that the rate of pit nucleation depends on the applied potential, suggesting the existence of nucleation sites of different energies which nucleate at distinct potentials. In other words, the more positive is the applied potential, the more will be the active sites available for pit nucleation. In addition, an increase in the applied potential may increase the electric field across the passive film and therefore enhances the adsorption of the Br^- anions.

Referring again to Fig. 1, it is observed in all cases that the electrode retains its passivity up to the pitting potential (E_{pit}) at which the passive current (j_{pass}) rises abruptly revealing initiation and growth of pitting (see region I). It is obvious that the pitting potential is shifted in the noble direction upon alloying TiNi alloy with Re. This positive shift in E_{pit} is more significant in presence of 0.3 Re than in presence of 0.1 Re. These results may indicate that the presence of Re, as an alloying element, in the tested alloy increases its pitting corrosion resistance, R_{pit}, and hence the rate of pitting corrosion decreased, to an extent depending on Re content. The numerical values of R_{pit} were calculated from the corresponding log j vs E plot of Fig. 1 (not shown here) based on the equation: $R_{pit} = |E_{corr} - E_{pit}|$, where E_{corr} is the corrosion potential.
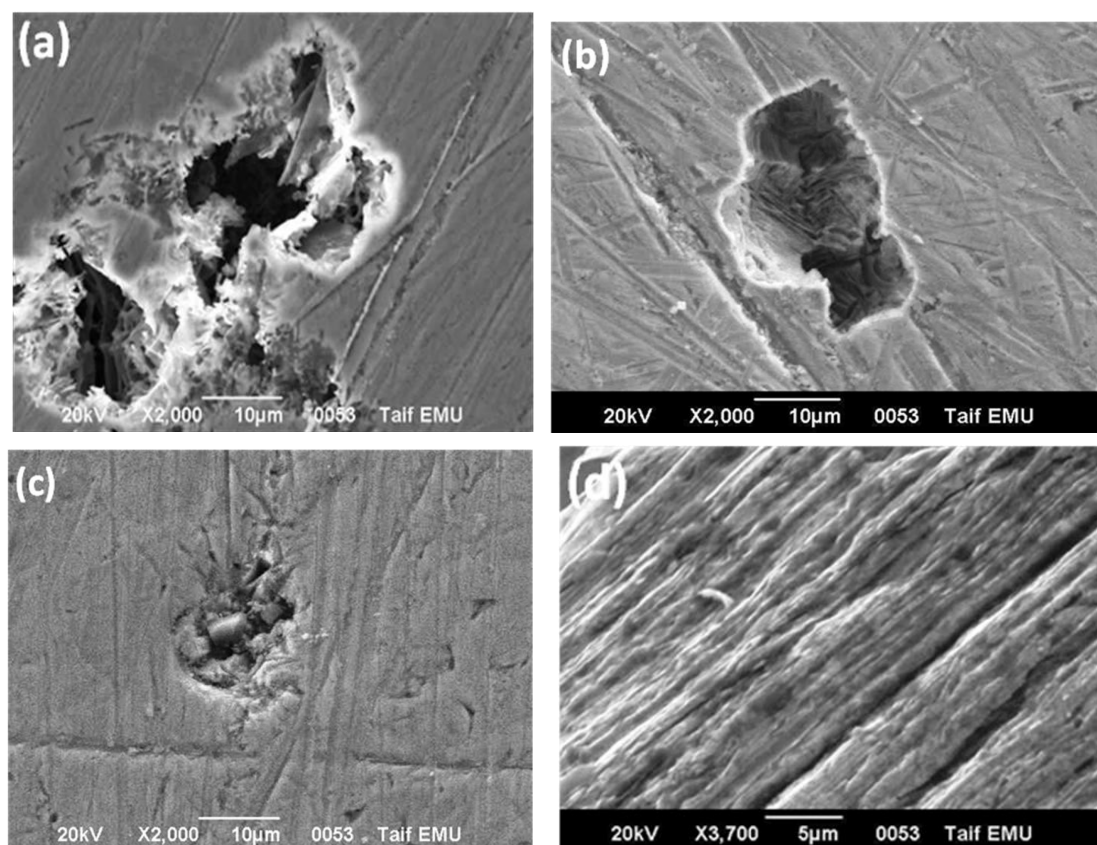
Figure 2. SEM micrographs recorded for pitted surfaces of (a) $Ti_{51}Ni_{49}$ alloy, (b) $Ti_{51}Ni_{49}Re_{0.1}$ alloy and (c) $Ti_{51}Ni_{49}Re_{0.3}$ alloy in 0.05 M KBr solution at 25 ^{o}C. Conditions of pitting attack; potentiostatic regime, where each alloy was held at a constant applied anodic potential, E_a, ($E_a > E_{pit}$ of any tested alloy) for 5.0 min. Image (d) is recorded for a passivated $Ti_{51}Ni_{49}$ alloy surface.

The suppression in the rate of pitting corrosion of the tested TiNi alloy with the increase in %Re in the alloy was further confirmed chemically using inductively coupled plasma-atomic emission spectroscopy (ICP-AES). This method of chemical analysis involved determination of Ni^{2+} ions in solution after each pitting corrosion test performed for studying pitting morphologies (see more details in the experimental part) as a function of alloy composition. The amount of nickel released into the corrosive medium, as a result of the aggressive attack of Br^-, was taken as a measure of the corrosion rate. Obtained results showed that $[Ni^{2+}]$ in solution obviously decreases upon alloying the tested alloy with Re. The $[Ni^{2+}]$ is always smaller in presence of 0.3 Re than in case of the 0.1 Re-SMA. Meaning that the rate of pitting corrosion suppresses with the percentage of the alloyed Re in the tested samples.

Pitting morphology studies came to the same conclusion, as shown in Figs. 2a-c which present morphologies of the pitted surfaces of the three tested SMAs in 0.05 M KBr solutions at 25 ^{o}C. These morphologies were recorded after exposing the samples to pitting attack under potentiostatic regime. Each electrode was held at a constant applied anodic potential, E_a, ($E_a > E_{pit}$ of any tested alloy) for 5.0 min.It was observed that no pitting phenomena occurred on the surfaces of the three tested alloys exposed to a potential negative to E_{pit} due to passivation (see image d that recorded for $Ti_{51}Ni_{49}$ alloy as a representative example). Almost similar morphologies were obtained for the passivated surfaces of the two tested Re-containing SMAs (such morphologies not included here). On the contrary, if the sample is polarized at fixed anodic potential beyond E_{pit}, passivity breakdown followed by initiation and propagation of pits occur, as shown in images a–c. In all cases, the formed pits are surrounded on all sides by the regions covered with oxide layer and corrosion products that accumulate around the edges of pits. It is obvious that, with increase in the alloyed Re, the pitted areas decrease. In other words, the areas of the protective oxide layer increase at the expense of the pitted ones with increase in alloyed Re. This means that the ratio of pitted area to total surface area (*i.e.*, pit area density) decreased with increase in Re content, corresponding to increased resistance against pitting. It follows from the micrograph depicted in image c that the severity of pitting attack is greatly suppressed in presence of 0.3 Re, with no corrosion products. This confirms that $Ti_{51}Ni_{48.7}Re_{0.3}$ alloy possesses the highest pitting corrosion resistance among the tested SMAs.

Upon reversing the scan into the cathodic direction, higher current is noticed corresponding to continued growth of pits even after scan reversal. This continued growth of pits even after scan reversal is seen only in case of $Ti_{51}Ni_{49}$ alloy (i.e., in absence of Re), as shown in region II, reflecting the higher pitting corrosion susceptibility of such alloy as compared with $Ti_{51}Ni_{48.9}Re_{0.1}$ and $Ti_{51}Ni_{48.7}Re_{0.3}$ shape memory alloys. This finding, as will be seen and fully discussed, confirms that alloying $Ti_{51}Ni_{49}$ with Re improves its resistance towards pitting attack.

Finally, a well-defined hysteresis loop is developed. The appearance of the hysteresis loop is typical of the pitting behaviour of metals [15]. Then pit growth is hindered due to repassivation of pit and current decreases gradually with decreasing the anodic potential. Finally, the decreasing current intersects the forward scan at a certain potential, known as the repassivation potential (E_{rp}), see region III [16]. The repassivation potential E_{rp} corresponds to the potential value below which no pitting occurs and above which pit nucleation begins [17]. The most important pitting corrosion parameters, namely E_{pit} and E_{rp} are well-defined in the insert of Fig. 1.

Charge passage measurements using software of the Autolab frequency response analyzer (General Purpose Electrochemical System, GPES, Version 4.9) showed that the total charge passed between E_{pit} and E_{rp} (i.e., after complete formation of the hysteresis loop) was 65×10^{-2}, 50×10^{-2}, and 27×10^{-2} C cm^{-2} for $Ti_{51}Ni_{49}$, $Ti_{51}Ni_{48.9}Re_{0.1}$ and $Ti_{51}Ni_{48.7}Re_{0.3}$ shape memory alloys, respectively. The high value of the charge consumed during hysteresis loop formation of $Ti_{51}Ni_{49}$ alloy suggests that $Ti_{51}Ni_{49}$ alloy finds it difficult to repassivate in this system, while $Ti_{51}Ni_{48.9}Re_{0.1}$ and $Ti_{51}Ni_{48.7}Re_{0.3}$ alloys tend to repassivate more easily. This means that $Ti_{51}Ni_{49}$ alloy suffers from severe pitting during the reverse scan much more than $Ti_{51}Ni_{48.9}Re_{0.1}$ and $Ti_{51}Ni_{48.7}Re_{0.3}$ alloys. The ease repassivation tendency of $Ti_{51}Ni_{48.7}Re_{0.3}$ alloy is undoubtedly due to the effect of Re as an alloying element, see later.

The linear current–potential relationship observed in region III for all samples suggests that an ohmic controlled process is taking place [18]. It is known that during the growing process of an occluded pit, the concentration of metallic cations increases gradually due to the active dissolution within the pit [18–20]. Once the saturated concentration is reached, a salt film will be formed at the bottom of the pit. The dissolved metallic cations move outward through the salt film under the action of electric field across the film. The stronger the field is, the faster the metallic cations move through the film. Hence, in this stage the growth of the pit is controlled by the ohmic potential drop across the salt film [18–20].

Pitting corrosion is a localized breakdown of the oxide film in which holes or pits are formed on the metal surface. It is initiated by adsorption of aggressive anions at the defective surface oxide film, resulting in the local breakdown of the oxide on the surface. Bromide, the present aggressive anion, acts in this manner; it adsorbs on the oxide/solution interface under the influence of electric field in competition with the passive layer forming species for active surface sites on the oxide [21].

Such adsorption of Br$^-$ anions is confirmed from the EDX spectra presented in Figs. 3a-c. This is clearly seen from the signal characteristic for Br. Therefore, it can be concluded that the passive film formed on the alloy surface contains a certain amount of incorporated Br. The atomic percentage of each element detected by EDX on the surfaces of the three tested samples is depicted in the tables under each EDX spectra. These tables were constructed based on ZAF Method Standardless Quantitative Analysis, covering the energy range (0–20 keV) at 20.0 kV and at a counting rate of 10 747 cps. The obtained EDX data indicated that the passivated and corroded surfaces at all locations (even inside pits) had the elemental composition Ti,Ni,O,C, and Br, in addition to Re in case of $Ti_{51}Ni_{48.9}Re_{0.1}$ and $Ti_{51}Ni_{48.7}Re_{0.3}$ alloys. It is obvious that the atomic percentage of Br is suppressed, and hence the rate of the aggressive attack of Br$^-$ anions is decreased, upon alloying TiNi alloy with Re. These findings confirm polarization measurements that Re, as an alloying element, improves the resistance of the tested samples towards pitting corrosion induced by the aggressive Br$^-$ anions.

This localized breakdown of the surface oxide film, induced by Br$^-$ anions in the present case, eventually exposes the underlying metal. Recent studies support the idea of oxide film removal via pitting corrosion to expose underlying reactive metal. Gaspar et al. [22] exposed zero-valent iron (Fe(0)) to water containing carbon tetrachloride (CCl_4) and examined the surface with Auger electron spectroscopy (AES) and time-of-flight secondary ion mass spectroscopy (ToF-SIMS) to map chemical distributions on the surface.
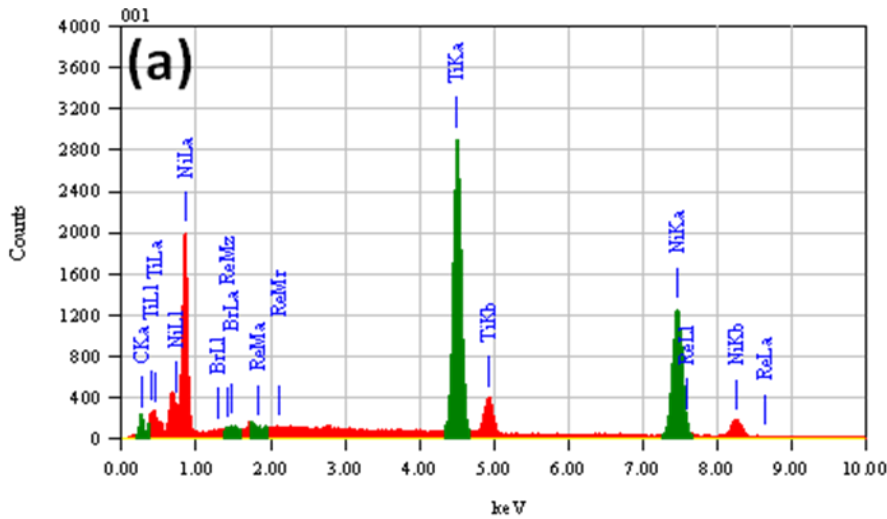
ZAF Method Standardless Quantitative Analysis
Fitting Coefficient : 0.2088

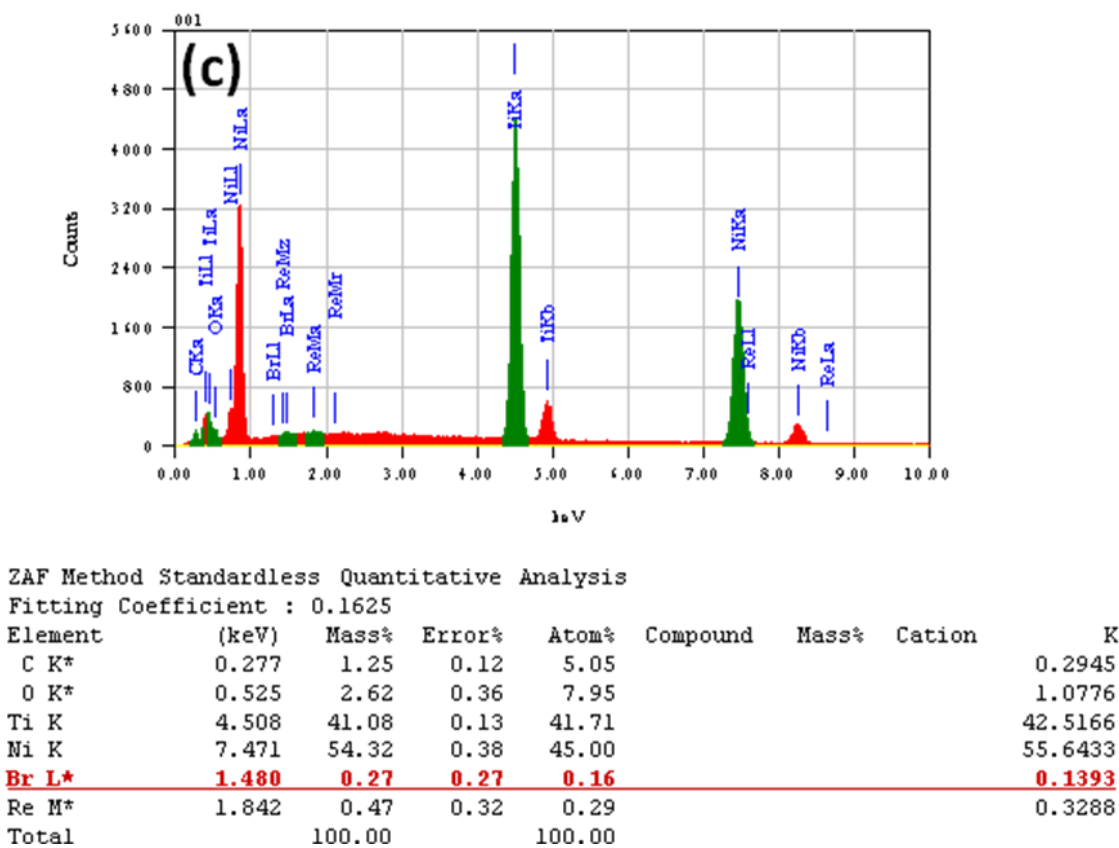| Element	(keV)	Mass%	Error%	Atom%	Compound	Mass%	Cation	K
C K	0.277	5.46	0.16	23.53				1.5795
Ti K	4.508	40.89	0.18	37.33				43.4372
Ni K	7.471	52.30	0.51	38.95				54.7959
Br L*	1.480	1.35	0.35	0.72				0.1874
Re M*								
Total		100.00		100.00				
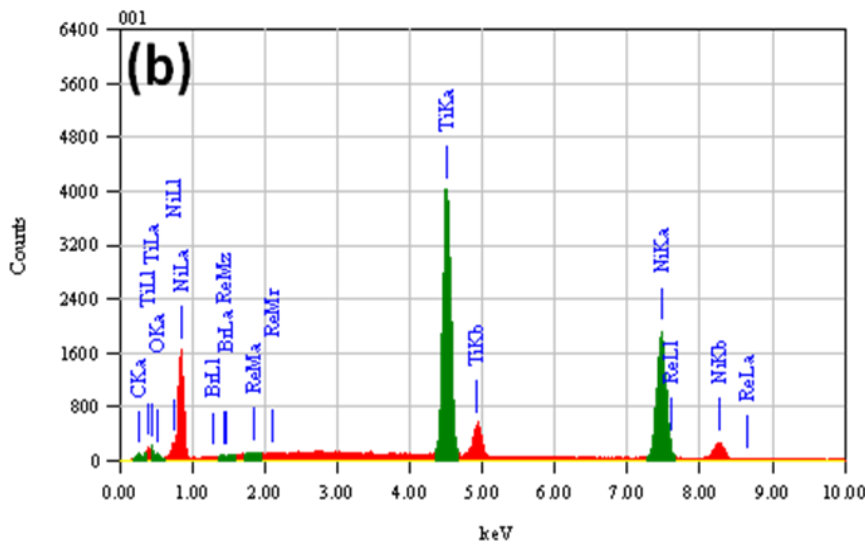
ZAF Method Standardless Quantitative Analysis
Fitting Coefficient : 0.1596

Element	(keV)	Mass%	Error%	Atom%	Compound	Mass%	Cation	K
C K*	0.277	0.80	0.12	3.39				0.1858
O K*	0.525	1.23	0.34	3.89				0.5030
Ti K	4.508	41.29	0.13	43.74				42.1226
Ni K	7.471	56.63	0.36	48.95				57.1541
Br L*	1.480	0.84	0.26	0.47				0.0166
Re M*	1.842	0.15	0.03	0.11				0.0179
Total		100.00		100.00				

```
ZAF Method Standardless Quantitative Analysis
Fitting Coefficient : 0.1625
Element      (keV)   Mass%   Error%   Atom%  Compound   Mass%  Cation          K
  C K*       0.277    1.25    0.12     5.05                                0.2945
  O K*       0.525    2.62    0.36     7.95                                1.0776
Ti K        4.508   41.08    0.13    41.71                               42.5166
Ni K        7.471   54.32    0.38    45.00                               55.6433
Br L*       1.480    0.27    0.27     0.16                                0.1393
Re M*       1.842    0.47    0.32     0.29                                0.3288
Total               100.00           100.00
```

Figure 3. EDX spectra and analysis recorded for the corresponding pitted surfaces presented in Fig. 2. **(a)** $Ti_{51}Ni_{49}$ alloy, **(b)** $Ti_{51}Ni_{49}Re_{0.1}$ alloy and **(c)** $Ti_{51}Ni_{49}Re_{0.3}$ alloy.

The chemical maps showed that high densities of elemental Cl and Cl^- existed at the area associated with pits on the surface of the Fe(0). This implies that pitting corrosion can effectively remove the oxide film and promote chemical reactions in localized areas by exposing the underlying metal or partially oxidized dissolved metal ions. Other studies have shown that pretreatment of zero-valent metals with solutions containing acids or chloride, promotes pitting corrosion [23]. Similar findings were also obtained in our previous study [24], during pitting corrosion studies of Zn in thiosulphate solutions, where high atomic % of elemental S (resulted from the adsorption of the aggressive $S_2O_3^{2-}$ anions) existed at the area associated with pits on the surface of Zn. This exposure of the underlying metal induces rapid metal dissolution at the localized pitting site and the dissolved metal ions undergo hydrolysis reactions that develop a high concentration of H^+ inside of the pit (autocatalytic nature of pitting) [15–17].

The role played by Re in enhancing R_{pit} of the tested TiNi alloy in these solutions may be explained on the basis that any localized dissolution will preferentially dissolve the alloy matrix (Martenzitic phase; detailed microstructure studies will be presented in a future complementary study), and leave the surface enriched in unreactive Re atoms.

Enrichment of alloy surface in unreactive Re atoms during dissolution blocks the active sites available for matrix dissolution. At this stage, dissolution is retarded and pitting ceases. In order for pitting to recommence, the potential must be raised even higher [to $(E_{pit})_{alloy}$] to activate dissolution at

the less favourable sites. As the Re content is increased from 0.1 to 0.3, Re atoms will appear with greater frequency.

Therefore, dissolution processes will be retarded until increasingly higher potentials are reached. Therefore, $(E_{pit})_{alloy}$ must increase with Re content, as shown in Fig. 1.

The high corrosion resistance of TiNiRe alloys may also be attributed to the incorporation of Re atoms in the alloy passive film. This incorporation may repair the film defects and precludes significant dissolution of the oxide film.

This makes it more difficult for Br^- ions to migrate through the passive oxide film. Re would as a result increase the difficulty of soluble film formation required for film rupture to occur [25]. Re may also slow down the rate of metal dissolution by reducing the amount of free metal ions in the pit solution resulting in a decrease in diffusion of Br^- into the pit and reduction in diffusion of metal cations out of the pit [26].

4. CONCLUSION

The electrochemical behavior of $(Ti_{51}Ni_{49-x}Re_x)$ shape memory alloys, SMAs, (x = 0, 0.1 and 0.3 %) have been studied in 0.05 M KBr solution based on cyclic polarization measurements, complemented with SEM/EDX examinations. cyclic polarization measurements revealed that the susceptibility of $Ti_{51}Ni_{49}$ alloy towards pitting attack was suppressed when the percentage of the alloyed Re was increased. The 0.3Re-containing SMA (i.e., $Ti_{51}Ni_{48.7}Re_{0.3}$ alloy) presented the highest corrosion resistance towards pitting corrosion in KBr solutions among the tested SMAs. Morphological studies of pitted surfaces, based on SEM examinations, revealed that the severity of pitting decreased with increase in alloyed Re content in the test samples. ICP-AES method of chemical analysis came to the same conclusion and confirmed polarization measurements and pitting morphology studies.

References

1. K. Otsuka, X. Ren, *Intermetallics*, 7 (1999) 511.
2. S. Miyazaki, Medical and dental applications of shape memory alloys. In: Otsuka K, Wayman C, Editors. Shape memory materials. Cambridge: Cambridge University Press; (1998), p. 267.
3. T. Duerig, A. Pelton, D. Stockel, *Mat. Sci. & Eng.* A, 273 (1999) 149.
4. D.D. Macdonald, *Pure Appl. Chem.*, 71 (1999) 951.
5. R.P. Frankenthal, J. Kruger (Eds.), Passivity of Metals, Electrochem. Soc. Princeton, NJ (1978), p. 165.
6. T.R. Beck, *J. Electrochem. Soc.*, 120 (1973) 1310.
7. T.P. Hoar, *Corros. Sci.*, 5 (1965) 279.
8. J. Kruger, *Int. Mater. Rev.*, 33 (1988) 113.
9. J. Stewart, D.E. Williams, *Corros. Sci.*, 33 (1992) 457.
10. G.S. Frankel, *J. Electrochem. Soc.*, 145 (1998) 2970.
11. S.Y. Yu, W.E. O'Grady, D.E. Ramaker, P.M. Natishan, *J. Electrochem. Soc.*, 147 (2000) 2952.
12. Z. Jiang, X. Dai, T. Norby, H. Middleton, *Corros. Sci.*, 53 (2011) 815.

13. Z. Jiang, T. Norby, H. Middleton, *Corros. Sci.*, 52 (2010) 3158.
14. A.D. Davydov, *Electrochim. Acta*, 46 (2001) 3777.
15. M. Metikos-Hukovic, *J. Appl. Electrochem.*, 22 (1992) 448.
16. H. Kaesche, Werk. *Korros.* 39 (1988) 152.
17. Z. Szklarska-Smialowska, Pitting Corrosion of Metals, NACE, Houston, TX (1986), p. 213.
18. A.G. Munoz, J.B. Bessone, *Corros. Sci.*, 41 (1999) 1447.
19. V. Moutarlier, M.P. Gigandet, *J. Pagetti, Appl. Surf. Sci.*, 206 (2003) 237.
20. Z. Szklarska-Smialowska, *Corros. Sci.*, 41 (1999) 1743.
21. L. Sziraki, A. Sziraki, I. Geroes, Z. Vertesy, L. Kiss, *Electrochim. Acta*, 43 (1998) 175.
22. D.J. Gaspar, A.S. Lea, M.H. Engelhard, D.R. Baer, R. Miehr, P.G. Tratnyek, *Langmuir*, 18 (2002) 7688.
23. R. Hernandez, M. Zappi, C.H. Kuo, *Environ. Sci.& Technol.*, 38 (2004) 5157.
24. S. S. Abd El-Rehim, E.Hamid, A. M. Shaltot, M. A. Amin, *Z. Phys. Chem.*, 225 (2011) 1–25 / DOI 10.1524/zpch.2011.0122.
25. R.T. Foley, *Corrosion*, 42 (1986) 277.
26. H. Bohni, *Langmiur*, 3 (1987) 924.